Macromolecules **1983**, *16*, 875–880

(7) Ito, T.; Shirakawa, H.; Ikeda, S. *J. Polym. Chem. Polym. Chem. Ed.* **1974**, *12*, 11.

(8) (a) Deits, W.; Cukor, P.; Rubner, M.; Jopson, H. *J. Electron. Mater.* **1981**, *10*, 683. (b) Sichel, E. K.; Knowles, M.; Rubner, M.; Georger, J., Jr. *Phys. Rev. B* **1982**, *25*, 5574.

(9) Baughman, R. H.; Hsu, S. L.; Pez, G. P.; Signorelli, A. J. *J. Chem. Phys.* **1978**, *68*, 5405.

(10) For polyacetylene, see: Shirakawa, H.; Ikeda, S. *Polym. J.* **1971**, *2*, 231. For polybutadiene, see: Haslam, J.; Willis, H. A. "Identification and Analysis of Plastics"; Van Nostrand: Princeton, NJ, 1965.

(11) Paul, D. R.; Newman, S. "Polymer Blends"; Academic Press: New York, 1978.

(12) Results to be published.

(13) Park, Y. M.; Druy, M. A.; Chiang, C. K.; MacDiarmid, A. G.; Heeger, A. J.; Shirakawa, H.; Ikeda, S. *J. Polym. Sci., Polym. Lett. Ed.* **1979**, *17*, 195.

(14) Fincher, C. R., Jr.; Peebles, D. L.; Heeger, A. J.; Druy, M. A.; Matsamura, Y.; MacDiarmid, A. G.; Shirakawa, H.; Ikeda, S. *Solid State Commun.* **1978**, *27*, 489.

Order in Nematic Phase of Semiflexible Polymers

Gilles Sigaud[†] and Do Y. Yoon*

IBM Research Laboratory, San Jose, California 95193

Anselm C. Griffin

Department of Chemistry, University of Southern Mississippi,
Hattiesburg, Mississippi 39401.

Received July 13, 1982

ABSTRACT: Orientational order in the nematic phase of the thermotropic aromatic polyester $(C_{10}H_{20}OC_6H_4COOC_6H_4OC_{10}H_{20}OC_6H_4OOCC_6H_4O)_x$ has been evaluated from magnetic susceptibility measurements and has been compared with those for the corresponding monomer and dimer, i.e., $C_5H_{11}O$-$C_6H_4COOC_6H_4OC_5H_{11}$ and $C_5H_{11}OC_6H_4COOC_6H_4OC_{10}H_{20}OC_6H_4OOCC_6H_4OC_5H_{11}$, respectively. The (orientational) order parameter of this polymer near the isotropic–nematic transition is found to be ca. 0.6, compared to the corresponding order parameters of ca. 0.4 for the monomer and ca. 0.5 for the dimer. These results are thus confirmatory of the recent theory of Ronca and Yoon, which predicts that the isotropic–nematic phase transition of semiflexible polymers does not entail a very high degree of order in the resultant nematic phase and that this nematic phase should become a thermodynamically viable state for polymers with limited flexibility. This finding is contrary to the ideas of polymer crystallization or glass transition advocated on the physical impossibility of random chains with limited flexibility to fill the space.

Introduction

The state of intermediate order, i.e., the nematic phase, of bulk polymers has been the subject of intesnse investigations in recent years from both experimental[1–6] and theoretical[7,8] standpoints. Although the discovery of the nematic phase of bulk polymers was rather recent, first by Roviello and Sirigue in 1975,[1] a large number of polymers have since been synthesized to exhibit nematic melts, and some of them are found to undergo isotropic–nematic phase transitions involving latent heat. Nematic polymers, upon processing, exhibit better chain orientation and improved mechanical properties than conventional polymers and, hence, are of great technological interest.[2]

From a fundamental theoretical point of view, the appearance of the nematic phase of bulk polymers present a new and challenging situation. The isotropic phase of bulk polymers wherein the polymer chains adopt *unperturbed random coil* configurations is now well established[9,10] in accordance with the predictions of the lattice theory of Flory.[11] However, in this theory the isotropic phase of random coils is predicated on the conditions that the polymer chains are sufficiently flexible. Thus, as the chain flexibility decreases, say with decreasing temperature, the isotropic phase of bulk polymers should become untenable.[7,12] The consequence of such limited flexibility, or semiflexibility, of random chains has been theorized to lead to a perfectly ordered state, i.e., crystalline order,[12,13] or glass transition,[14] when the crystalline order is inhibited, due to the vanishing configurational entropy of random chains. This is shown schematically in Figure 1 in terms of relative free energy of the isotropic phase vs. temperature, wherein T_c and T_2 (T_g) denote the temperatures of crystallization[12] and glass transition[14] thus predicted.

In these theories, however, the state of intermediate order has not been considered. The possibility that the untenability of the isotropic phase of semiflexible polymers will result in a first-order transition to an ordered state was recognized early by Flory.[12] But it is only very recently that a detailed theory of nematic systems of semiflexible polymers was developed by Ronca and Yoon.[8] According to this theory, the consequence of this limited flexibility of bulk polymers should lead to the transition of the isotropic phase into a nematic phase containing considerable disorder. This is shown schematically in Figure 1 by the intersection of the free energy curve of the nematic phase with that of the isotropic phase. Therefore, the degree of conformational and orientational order in the nematic phase thus formed is predicted to be not very high, with the orientational order parrameters at the transition falling in the range 0.4–0.7.

It is the intent of this paper to test the basic premise of this theory of Ronca and Yoon that the isotropic–nematic transition of semiflexible polymers does not entail a very high degree of orientational order in the resultant nematic phase. The subject of conformational order is touched upon only briefly here and will be discussed in detail in a separate paper.[15]

For this purpose we chose the thermotropic polyester $(C_{10}H_{20}OC_6H_4COOC_6H_4OC_{10}H_{20}OC_6H_4OOCC_6H_4O)_x$ (I), shown schematically in Figure 2a, because of its relatively low isotropic–nematic transition temperature $T_{NI} \simeq 215$ °C and the resultant thermal stability of the polymer in the nematic state. A detailed study of the thermal properties of this class of thermotropic polymers and the

---

[†] IBM World Trade Postdoctoral Fellow. Permanent address: Centre de Recherche Paul Pascal Domaine Universitaire, 33405 Talence, France.

0024-9297/83/2216-0875$01.50/0

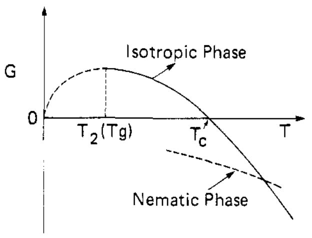

Figure 1. Schematic represenation of free energy of semiflexible polymers in the bulk vs. temperature for the isotropic phase of random chains calculated from the Flory–Huggins lattice model and that for the nematic phase around the isotropic–nematic transition from the theory of Ronca and Yoon.[8] T_c and T_2 (T_g) denote the temperatures of crystallization[12] and glass transition[14] prediced for the isotropic phase from the lattice model.

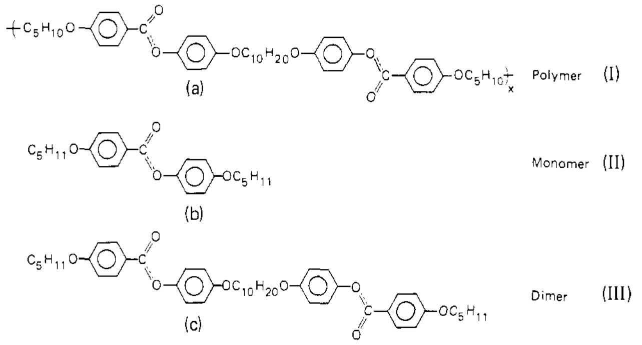

Figure 2. (a) Schematic diagram of the polymer (I), (b) the corresponding monomer (II), and (c) the corresponding dimer (III).

identification of the nematic phase of these polymers have been reported previously.[4] For the purpose of comparing with classical thermotropic liquid crystals, we also chose the compound $C_5H_{11}OC_6H_4COOC_6H_4OC_5H_{11}$ (II), shown schematically in Figure 2b, i.e., a monomeric analogue of the polymer (I) in terms of its rigid and flexible sections, and the corresponding dimer $C_5H_{11}OC_6H_4COOC_6H_4O\text{-}C_{10}H_{20}OC_6H_4OOCC_6H_4OC_5H_{11}$ (III), shown in Figure 2c.

The (orientational) order parameter s of interest here is defined by

$$s = (3\langle\cos^2\phi\rangle - 1)/2 \tag{1}$$

where ϕ is the angle between the chain segment and the orientation axis of the domain and the brackets represent the averaging over all the chain segments within the domain. These order parameters were evaluated from the measurements of diamagnetic anisotropy $\Delta\chi$ through the relationships[16]

$$\Delta\chi = \chi_\parallel - \chi_\perp = {}^3/_2(\chi_\parallel - \bar{\chi}) \tag{2}$$

$$= \Delta\chi_0 s \tag{3}$$

where $\chi_\parallel$ and $\chi_\perp$ are the magnetic susceptibilities along and perpendicular to the domain axis, respectively, the mean susceptibility $\bar{\chi} = (\chi_\parallel + 2\chi_\perp)/3$ for uniaxial orientation, and $\Delta\chi_0$ is the diamagnetic anisotropy of the chain segment, i.e., the diamagnetic anisotropy for the system of perfect orientational order ($s = 1$). Except for the negligible effects of chain ends, the value of $\Delta\chi_0$ is thus independent of chain length at a given temperature as long as the axis of perfect orientational order does not change with chain length.

Experimental Section

Materials. The polymer was prepared by interfacial polyesterification of 1,10-bis[4-(chloroformyl)phenoxy]decane and 1,10-bis(4-hydroxyphenoxy)decane.[4] The molecular weight of the polymer was not determined separately, but its inherent viscosity in 60:40 (v/v) phenol–tetrachloroethane was measured to be ~0.8 dL/g, thus indicating a reasonably high molecular weight, and this value was found to remain relatively unchanged for polymer samples subjected to prolonged exposure at 240 °C.[17] The dimer was prepared by reaction of 4-(pentyloxy)benzoic acid with 1,10-bis(hydroxyphenoxy)decane according to the general method of Hassner and Alexanian.[18] The monomer was prepared by the reaction of 4-(pentyloxy)benzoyl chloride and 4-(pentyloxy)phenol according to the method of van Meter and Klanderman.[19]

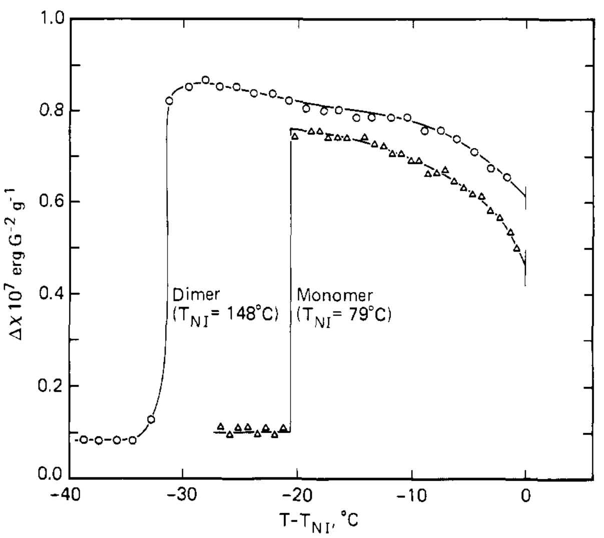

Figure 3. Diamagnetic anisotropy $\Delta\chi$ of the monomer and the dimer as a function of temperature around the isotropic–nematic transition. Measurements were made under a field of 20 kG and at cooling rates of 0.13 °C/min for the monomer and 0.25 °C/min for the dimer.

All the samples were dried in a vacuum oven at 100 °C for 2 days to remove the residual solvents before the susceptibility measurements. During the measurements the samples were kept under a helium atmosphere.

Magnetic Susceptibility Measurements. We used a Faraday balance, which has a maximum field B_{max} = 20 kG and a maximum field gradient $\partial B/\partial x$ = 180 G cm^{-1} produced by two Lewis coils. The balance has an accuracy to ~0.1 μg, and the field and the field gradient are measured within 0.1% accuracy.[20] Samples of about 50 mg were used to generate a total magnetic force of ~500 μg.

In this method, the magnetic susceptibility χ is determined along the field axis from the measured magnetic force F acting on the induced magnetic moment in a given field gradient by

$$F = mB\frac{\partial B}{\partial x}\chi \tag{4}$$

where m is the sample mass. For nematic systems, the applied field can be made strong enough to align all the domains along the field, thereby yielding a measured susceptibility corresponding to the susceptibility along the domain axis, i.e., $\chi_\parallel$ in eq 2. On the other hand, measurements in the isotropic phase correspond to the mean susceptibility $\bar{\chi}$ in the same equation.

Calorimetric Measurements. All the calorimetric measurements were carried out with a DuPont 990 differential scanning calorimeter (DSC) employing a cooling rate of 1 °C/min. Each DSC run was calibrated with indium standard and each peak area was measured with a planimeter and averaged over ten separate measurements.

Results

Monomer (II) and Dimer (III). The diamagnetic anisotropies $\Delta\chi$ for the monomer and the dimer are shown in Figure 3 as a function of temperature. For these measurements the samples were initially heated to ~10 °C above the isotropic–nematic transition temperature of T_{NI} = 79 °C for the monomer and T_{NI} = 148 °C for the dimer. Then the samples were cooled down under an applied field of 20 kG at constant cooling rates of 0.13 and 0.25 °C/min for the monomer and the dimer, respectively. The mag-

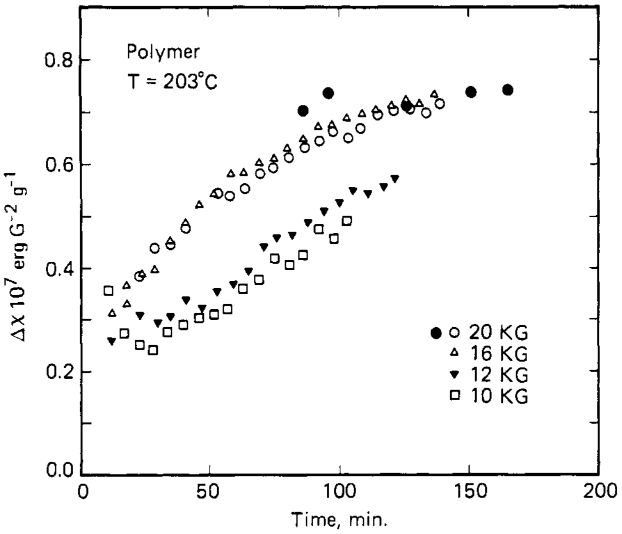

Figure 4. Change in diamagnetic anisotropy of the polymer at 203 °C with time under various applied field strengths. The open and filled circles both represent measurements with 20-kG field, using manual data recording (filled circles) and computerized data collection averaged over 10 readings during every 6-min interval (open circles), respectively. All the other points were obtained with computerized data collection.

netic force was averaged for a period of 6 min and recorded at every 6-min interval. For these oligomeric compounds orientation of the nematic domains is quite rapid and, hence, the cooling rate is more than sufficient to allow complete alignment of all the nematic domains under the applied magnetic field.

The abrupt increase of $\Delta\chi$ at the isotropic–nematic transition, its continuing increase with decreasing temperature, and its sharp decrease upon crystallization for these oligomeric model compounds follow closely the general characteristics observed for classical liquid crystals, e.g., *p*-azoxyanisole (PAA) and *p*-(*p*-methoxybenzylidene)(aminobutyl)benzene (MBBA).[16] The dimer, however, seems to exhibit a more gradual increase of $\Delta\chi$ with decreasing temperature than those exhibited by the monomer and other "monomeric" liquid crystals such as PAA and MBBA. Furthermore, the dimer shows a considerably larger value of $\Delta\chi$ at the isotropic–nematic transition (and hence a higher order parameter), $\Delta\chi_{\mathrm{NI}} \simeq 0.61 \times 10^{-7}$ erg G^{-1} g^{-1}, than that for the monomer, for which $\Delta\chi_{\mathrm{NI}} \simeq 0.46 \times 10^{-7}$ erg G^{-2} g^{-1}.

Polymer (I). Due to the much longer relaxation times resulting from the long chain lengths, orientation of nematic domains of bulk polymers is much slower and requires a much higher field than those for oligomeric liquid crystals. Hence, in order to ensure that we can achieve complete alignment of nematic domains of the polymer under our experimental conditions, we first measured the diamagnetic anisotropy $\Delta\chi$ as a function of time under various field strengths from 10 to 20 kG as shown in Figure 4. For these measurements the polymer samples were initially heated to ~225 °C, which is ~10 °C above the nematic–isotropic transition point of the polymer. The samples were then cooled to 203 °C and subsequently were subjected to a given magnetic field. To prevent complications from possible thermal degradation of the polymer, measurements at each field were started with new samples.

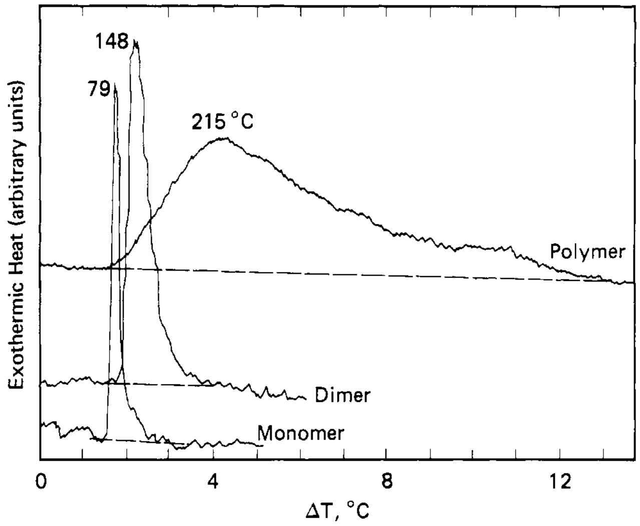

Figure 5. DSC traces in arbitrary units near the isotropic–nematic transition of the monomer, the dimer, and the polymer while the sample was cooled at 1 °C/min. The peak temperatures are identified in the figure for each sample.

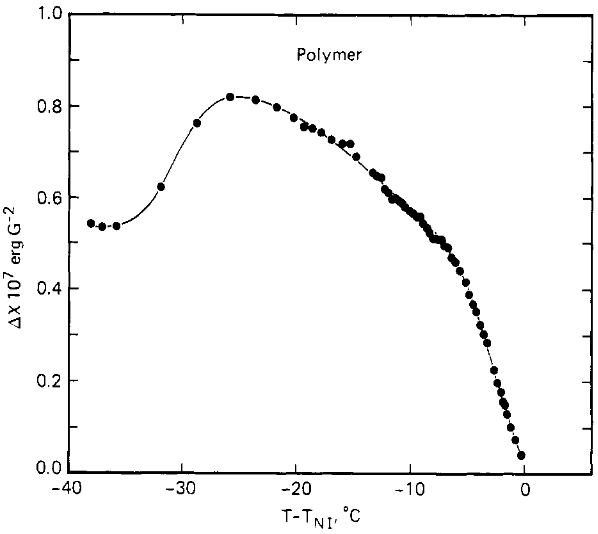

Figure 6. Diamagnetic anisotropy $\Delta\chi$ of the polymer as a function of temperature. The measurements were carried out while the sample was cooled at the rate of 0.08 °C/min starting from ~225 °C under a field of 20 kG. T_{NI} denotes the incipient temperature of transition 217 °C as shown in Figure 5.

Another difference from the oligomeric liquid crystals is that the nematic–isotropic transition of the polymer occurs over a very broad temperature range; the transition takes place over an interval of ~12 °C, compared to 1–2 °C for the monomer and the dimer as shown by the DSC traces in Figure 5. Hence, the temperature of 203 °C was chosen to ensure that the transition is completed. Since this will introduce the effect of supercooling on those portions of the sample that undergo the transition at temperatures higher than 203 °C, the measurements thus carried out at 203 °C will tend to *overestimate* the true order parameter at the transition.

The results in Figure 4 show that orientation of nematic domains of the polymer is indeed a very slow process. However, with fields of 20 kG (open and closed circles) and 16 kG (open triangle) an asymptotic limit of $\Delta\chi$ is reached in ~150 min. Furthermore, the fact that the asymptotic values of $\Delta\chi$ thus obtained are almost identical for the fields of 20 and 16 kG shows that field strengths ≥16 kG are sufficiently high to reach saturation. With fields of 12 kG (filled triangle) and 10 kG (open square), however, much longer times seem to be required.

Due to the long orientation time of the polymer the temperature dependence of $\Delta\chi$ of the polymer (Figure 6) was measured at the very slow cooling rate of 0.08 °C/min under a field of 20 kG. The change of $\Delta\chi$ with temperature

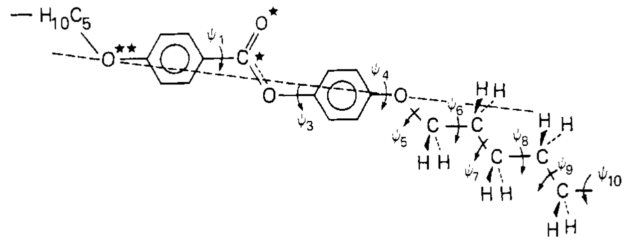

Figure 7. Schematic representation of the segment unit with the alkyl groups C_5H_{10} in all-trans conformation. The dashed line represents the segment axis.

around the incipient isotropic–nematic transition at ~217 °C is much more gradual than those for the monomer and the dimer, reflecting both the kinetic constraints and the breadth of the transition temperature interval of the polymer. The decrease in $\Delta\chi$ with the nematic–crystalline transition of the polymer around 190 °C is also found to be much more gradual than those of the monomer and the dimer (see Figure 3).

The reason for the broad temperature interval of the isotropic–nematic transition of the polymer remains uncertain. At the moment there exist two different possibilities: (i) biphasic separation due to polydispersity of chain lengths[21] and (ii) kinetic control analogous to crystallization of polymer melts.[22] Further experiments utilizing molecular weight fractions seem certainly required to provide further insight into the mechanisms of the isotropic–nematic transition of polymer melts.

Evaluation of Diamagnetic Anisotropy of Chain Segment

Evaluation of the order parameter s from the diamagnetic anisotropy $\Delta\chi$ according to eq 2 and 3 requires the value of the diamagnetic anisotropy of the chain segment, $\Delta\chi_0$. According to Flygare,[23] the magnetic susceptibility tensor of a given molecule can be evaluated quite accurately as the sum of the magnetic susceptibility tensor of each bond or group. Hence, the required value of $\Delta\chi_0$ was calculated for the segment $-C_5H_{10}OC_6H_4COOC_6H_4OC_5H_{10}-$ shown schematically in Figure 7.

In view of the twofold symmetry of the alkyl group arrangements around the phenylene–oxygen bond the axis of the chain segment was taken along the line connecting the two oxygen atoms adjoining the phenyl benzoate moiety as shown by the dashed line in Figure 7. For the dimer and the polymer, this implies that this is the axis of perfect orientational order (s = 1); that is, collinear alignments of adjoining phenyl benzoate units would not be impeded by the intervening alkyl groups. For the $C_{10}H_{20}$ group of interest here, this is certainly the case, as can be demonstrated, for example, by the all-trans conformation. Thus, the magnetic susceptibility tensor was computed in the reference frame of this axis (a axis) and the two orthogonal axes (b and c axes) normal to this axis. The diamagnetic anisotropy of the segment, $\Delta\chi_0$, was then computed as the difference between the segment-axis susceptibility, χ_{aa}, and the average of the two normal-axis susceptibilities, $(\chi_{bb} + \chi_{cc})/2$.

For simplicity in numerical computations, the calculations were first carried for the susceptibility tensor χ_{I} for the $OC_6H_4COOC_6H_4OC_5H_{10}$ group and χ_{II} for $OC_6H_4COOC_6H_4O$ group, starting from the O**–C* bond in Figure 7. The contribution χ_{III} of the other OC_5H_{10} group (on the left side of Figure 7) was then taken as $\chi_{\mathrm{I}} - \chi_{\mathrm{II}}$, and the total magnetic susceptibility tensor of the segment was computed as the sum of χ_{I} and χ_{III}.

The values of the susceptibilities along the principal inertia axes, χ_{11}, χ_{22}, and χ_{33}, of each bond considered here were taken from the tabulations of Flygare and are listed in Table I. For the benzene ring C_6H_4 in the chain

Table I
Bond or Group Susceptibilities along the Principal Inertia Axes[a]

	χ_{11}	χ_{22}	χ_{33}
benzene[b]	−34.9	−34.9	−94.6
C=O[c]	−1.3	2.2	−13.0
C–O[d]	−7.2	−6.7	−3.8
C–C[e]	−7.9	−0.2	−0.2
C–H[e]	−5.6	−3.1	−3.1

[a] In units of 10^{-6} erg G^{-2} mol^{-1}; from ref 20. [b] Axes 1, and 2 are in the plane of the ring. [c] Axis 1 is along the bond and axis 2 is in the plane of the pendant bonds. [d] Axis 1 is along the bond and axis 2 is in the plane of the bond pair adjoined to O. [e] Axis 1 is along the bond.

Table II
Bond Angles[a]

bond angle	angle, deg	bond angle	angle, deg
C^{ar}–C*–O*	124	C^{ar}–C^{ar}–C^{ar}	120
C^{ar}–C*–O	111	C^{ar}–C^{ar}–H	120
C*–O–C^{ar}	118	C–C–C	112
C^{ar}–O–C	112	C–C–H	110

[a] See Figure 7 for atom designation.

$$\chi_{C_6H_4} = \chi_{\mathrm{benzene}} - 2\chi_{\mathrm{C-H}} = \mathrm{diag}\,(-23.7, -28.7, -88.4)$$

in 10^{-6} erg G^{-1} mol^{-1}.

The bond geometries employed here were taken mostly from the tabulations of crystal structures of phenyl benzoate[24] and are listed in Table II. The ester group is in the planar-trans conformation ($\psi_2 = 0$), and the torsional angles ψ_1 and ψ_3 in Figure 7 were taken to be $\psi_1 = \pm 6°$ and $\psi_3 = \pm 65°$ as averages of crystalline aromatic esters.[25] Electron delocalization at the phenylene–oxygen bond enforces coplanarity of the phenylene–O–CH_2 bonds,[26] i.e., $\psi_4 = 0$ or 180°, and the consequent steric interactions result in preclusion of the gauche conformations of the O–CH_2 bond; hence, $\psi_5 = 0$.

The transformation of the magnetic susceptibility tensors of all the bonds and the groups of the segment and their summation in the reference frame of the segment axis can be accomplished by using the matrix multiplication method devised by Jernigan and Flory.[27-29] Thus, for a given spatial configuration of the segment comprising t skeletal bonds as specified by skeletal bond angles $\pi - \theta_i$ and the torsional angles ψ_i for each internal skeletal bond i, the segment magnetic susceptibility tensor in column form χ^c is given by

$$\chi^c = \mathbf{S}_{[0}\mathbf{S}_1^{(t-1)}\mathbf{S}_{t]} \tag{5}$$

where $\mathbf{S}_1^{(t-1)}$ stands for the serial product of the $t - 1$ generator matrices $\mathbf{S}_i$ commencing with $\mathbf{S}_1$ for bond 1 and the generator matrices $\mathbf{S}$ are

$$S_{[0} = [T \otimes T \quad 0]_0 \tag{6}$$

$$S_i = \begin{bmatrix} T \otimes T & \chi^c \\ 0 & 1 \end{bmatrix}_i \tag{7}$$

$$S_{t]} = \begin{bmatrix} \chi^c \\ 1 \end{bmatrix}_t \tag{8}$$

As defined previously,[28] $\mathbf{T}_i$ is the transformation for the reference frame for bond $i + 1$ to that for bond i and is

Table III
Diamagnetic Anisotropy, Order Parameter, Transition Enthalpy, and Transition Entropy at the Isotropic-Nematic Transition

	T_{NI}, °C	ΔH_{NI},[a] kJ mol^{-1}	ΔS_{NI},[a] J mol^{-1} K^{-1}	$10^7 \Delta\chi_{NI}$, erg G^{-2} g^{-1}	s_{NI}[b]
monomer (II)	79	0.74	2.09	0.46	0.37
dimer (III)	148	3.52	8.37	0.61	0.49
polymer (I)	~215	6.53	13.4	0.75[c]	0.60[c]

[a] Normalized per mole of segment unit of Figure 7. [b] Evaluated taking $\Delta\chi_0 = 1.25 \times 10^{-7}$ erg G^{-2} g^{-1}. [c] This represents an upper bound, since the measurements were carried out at 203 °C in order to ensure completion of the broad transition occurring over the ~12 °C interval.

a function of θ_i and ψ_i. $\mathbf{T}_0$ is the transformation of the reference frame for the first bond (O**–C* in Figure 7; see below) to that of the segment (hence, $\theta_0 = 9.3°$ and $\psi_0 = 0°$), and $\mathbf{T} \otimes \mathbf{T}$ denotes the self-direct product. χ_i^c denotes the column-form representation of susceptibility tensors summed over each bond or group that is grouped with skeletal bond rotation ψ_i and expressed in the reference frame for bond i. That is

$$\chi_1 = \chi_{O-C} + \chi_{C_6H_4} + \chi_{C-C}$$

$$\chi_2 = \chi_{C=O} + \chi_{C-O}$$

$$\chi_3 = \chi_5 = \chi_{O-C}$$

$$\chi_4 = \chi_{C_6H_4} + \chi_{C-O}$$

$$\chi_{6,7,8,9} = \chi_{C-C} + 2\chi_{C-H}$$

$$\chi_{10}{}^{30} \simeq \tfrac{1}{2}\chi_{C-C} + 2\chi_{C-H}$$

Effect of Alkyl Group Conformations on $\Delta\chi_0$. While the contributions from the rigid part $OC_6H_4COOC_6H_4O$ to $\Delta\chi_0$ is straightforward, the contribution of the alkyl groups is not clear, since their conformation (ψ_6, ψ_7, ψ_8, and ψ_9 in Figure 7) in the nematic phase is not known accurately. Strong even–odd effects of the number of alkyl CH_2 units on the isotropic–nematic transition temperatures[4] are suggestive of perference of the trans conformation. In view of this uncertainty $\Delta\chi_0$ was evaluated for two extreme cases of alkyl group conformations: (i) unperturbed random coil conformations of *n*-alkane chains[28,31] comprising trans (t), gauche$^+$ (g$^+$), and gauche$^-$ (g$^-$) conformations at $\psi = 0, \pm 120°$ and (ii) the completely ordered all-trans conformation.

The statistical mechanical averaging of χ given by eq 5 over all accessible configurations is easily amenable by the matrix multiplication method[28,29] employing the statistical weight matrix U. Hence, the average susceptibility tensor $\langle\chi_I{}^c\rangle$ of the $OC_6H_4COOC_6H_4OC_5H_{10}$ group in Figure 7 can be calculated by

$$\langle\chi_I{}^c\rangle = Z_I{}^{-1}\mathbf{S}_{[0}\langle\mathbf{S}_1\rangle\mathbf{S}_2\langle\mathbf{S}_3\rangle\langle\mathbf{S}_4\rangle\mathcal{S}_5\mathcal{S}_6\mathcal{S}_7\mathcal{S}_8\mathcal{S}_9\mathcal{S}_{10]} \quad (9)$$

where $Z_I{}^{-1}$ is the configurational partition function given by

$$Z_I = U_5U_6U_7U_8U_9U_{10} \quad (10)$$

$$U_5 = [1 \quad 0 \quad 0] \quad (11)$$

$$U_i = \begin{bmatrix} 1 & \sigma & \sigma \\ 1 & \sigma & \sigma\omega \\ 1 & \sigma\omega & \sigma \end{bmatrix}, \qquad 6 \leqslant i \leqslant 9 \quad (12)$$

$$U_{10} = \begin{bmatrix} 1 \\ 1 \\ 1 \end{bmatrix} \quad (13)$$

The brackets in $\langle\mathbf{S}_1\rangle$, $\langle\mathbf{S}_3\rangle$, and $\langle\mathbf{S}_4\rangle$ represent the averaging of $\mathbf{T} \otimes \mathbf{T}$ in eq 7 over the two torsional angles for each bond, $\psi_1 = \pm 6°$, $\psi_3 = \pm 65°$, and $\psi_4 = 0$ and $180°$, respectively, and

$$\mathcal{S}_5 = [\mathrm{S}(t) \quad 0 \quad 0]_5 \quad (14)$$

$$\mathcal{S}_i = \begin{bmatrix} u_{11}\mathrm{S}(t) & u_{12}\mathrm{S}(g^+) & u_{13}\mathrm{S}(g^-) \\ u_{21}\mathrm{S}(t) & u_{22}\mathrm{S}(g^+) & u_{23}\mathrm{S}(g^-) \\ u_{31}\mathrm{S}(t) & u_{32}\mathrm{S}(g^+) & u_{33}\mathrm{S}(g^-) \end{bmatrix}_i, \qquad 6 \leqslant i \leqslant 9 \quad (15)$$

$$\mathcal{S}_{10]} = \begin{bmatrix} \mathrm{S}_{10]} \\ \mathrm{S}_{10]} \\ \mathrm{S}_{10]} \end{bmatrix} \quad (16)$$

where u_{ij} denotes the elements of the statistical weight matrix $\mathbf{U}_i$ of eq 12.

Similarly, the average susceptibility tensor $\langle\chi_{II}{}^c\rangle$ of the $OC_6H_4COOC_6H_4O$ group is given by

$$\langle\chi_{II}{}^c\rangle = \mathbf{S}_{[0}\langle\mathbf{S}_1\rangle\mathbf{S}_2\langle\mathbf{S}_3\rangle\mathbf{S}_{4]} \quad (17)$$

For the case of random coil conformation of alkyl groups (case i), taking the statistical weights of $\sigma = 0.54$ and $\omega = 0.088$ for *n*-alkanes at 140 °C,[28,31] we obtain the value of the segment diamagnetic anisotropy $\Delta\chi_0 = 1.32 \times 10^{-7}$ erg G^{-2} g^{-1}, and for the case of all-*trans* conformation (case ii) $\Delta\chi_0 = 1.19 \times 10^{-7}$ erg G^{-2} g^{-1}. Considering that the difference in $\Delta\chi_0$ between these two extremes is rather small and that neither of these extremes is feasible in reality, it seems reasonable to assume that $\Delta\chi_0 \approx 1.25 \times 10^{-7}$ erg G^{-2} g^{-1}, regardless of chain length and temperature here. The error thus involved should not exceed 5%.

For comparison, if the alkyl group contributions are completely neglected, the resultant segment diamagnetic anistropy is found to be $\Delta\chi_0 = 1.60 \times 10^{-7}$ erg G^{-2} g^{-1} and, thus, demonstrates the importance of including the alkyl group susceptibilities.

Order Parameter at the Isotropic-Nematic Transition

The order parameters at the isotropic–nematic transitions thus evaluated by taking $\Delta\chi_0 = 1.25 \times 10^{-7}$ erg G^{-2} g^{-1} are shown in Table III for the monomer, the dimer, and the polymer together with their values of $\Delta\chi_{NI}$ at the transitions. The values of $\Delta\chi_{NI}$ for the monomer and the dimer were taken by extrapolating the results in Figure 3 to their respective transition points. The value for the polymer was taken from the asymptote of Figure 4. Also shown in the same table are the transition enthalpy ΔH_{NI} and transition entropy ΔS_{NI} of the nematic–isotropic transition of these compounds.

The value of the order parameter of the monomer at the transition, $s_{NI} \approx 0.37$, is found to be in good agreement with the values reported for other monomeric nematogens; e.g., $s_{NI} = 0.35$–0.40 for PAA obtained from ^{13}C NMR[32] and D NMR[33] measurements. The value of the order parameter exhibits a considerable increase to $s_{NI} \approx 0.49$ for the dimer and seems to increase further for the polymer. The value of $s_{NI} \approx 0.60$ for the polymer listed in Table III, however, represents an upper bound since the measurements were carried out at 203 °C, ~12 °C below the peak transition temperature, in order to ensure completion of broad transition as discussed above.

The transition enthalpy ΔH_{NI} and transition entropy ΔS_{NI} exhibits a much more marked increase with chain length than is expected from the order parameter according to[34] $\Delta H \propto s^2$. This indicates a much higher conformational order in the alkyl groups of the polymer in the nematic phase and is consistent with the strong even–odd effect of alkyl groups on the isotropic–nematic transition temperatures.[4] A detailed discussion on the conformational order accompanying the isotropic–nematic transitions of semiflexible polymers will be presented separately.[15]

Discussion

The order parameter of the nematic phase at the isotropic–nematic transition has been found to increase with chain length. However, the value of $s_{NI} \approx 0.60$ found as an upper bound for the polymer, while considerably larger than that for the monomer ($s_{NI} \approx 0.37$), does not represent a very high degree of order. Hence, this finding is confirmatory of the recent theory of Ronca and Yoon[8] on nematic systems of semiflexible polymers. Both the theory and the experiments thus show that the *intermediately ordered* nematic phase of semiflexible polymers is a thermodynamically viable state. Therefore, on purely thermodynamic grounds the isotropic phase of random chains should undergo a first-order transition into the nematic phase of intermediate order upon decreasing chain flexibiltiy.

This conclusion is contrary to the ideas that emphasize the physical impossibility of random chains with limited flexibility to fill the space as the primary thermodynamic cause for crystallization[12,13] or glass transition[14] of polymers. The isotropic–crystalline phase transition of polymers should be assisted greatly by intermolecular attractions to compete and intercept the isotropic–nematic transition. The thermodynamic theory of polymer glass transition, if it is valid, seems to require an explanation how the thermodynamically driven isotropic–nematic transition of polymers can be inhibited.

Acknowledgment. We are indebted to C. Pike and C. Scott for making available the Faraday balance and providing assistance with the measurements. G. Sigaud thanks IBM World Trade of France for providing a postdoctoral fellowship. This work was supported in part by a grant to A.C.G. from the National Science Foundation (DMR-8115703).

Registry No. I, 70857-27-1; II, 50649-42-8; III, 78352-90-6; 1,10-bis[4-(chloroformyl)phenoxy]decane-1,10-bis(4-hydroxyphenoxy)decane copolymer, 70856-66-5.

References and Notes

(1) Roviello, A.; Sirigue, A. *J. Polym. Sci., Polym. Lett. Ed.* **1975**, *13*, 455. *Eur. Polym. J.* **1979**, *15*, 61.
(2) Jackson, W. J., Jr.; Kuhfuss, H. F. *J. Polym. Sci., Polym. Chem. Ed.* **1976**, *14*, 2043.
(3) Nöel, C.; Monnerie, L.; Archard, M. F.; Hardouin, F.; Sigaud, G.; Gasparoux, H. *Polymer* **1981**, *22*, 578 and references therein.
(4) Griffin, A. C.; Havens, S. J. *J. Polym. Sci., Polym. Phys. Ed.* **1981**, *19*, 951. *J. Polym. Sci., Polym. Lett. Ed.* **1980**, *18*, 259.
(5) Jin, J. I.; Antoun, S.; Ober, C.; Lenz, R. W. *Br. Polym. J.* **1980**, *12*, 132.
(6) For recent reviews, see: (a) Blumstein, A. *Polym. News* **1979**, 5, 254. (b) Samulski, E. T.; DuPre, D. B. In *Adv. Liq. Cryst.* **1979**, *4*.
(7) Flory, P. J. *Proc. Natl. Acad. Sci. U.S.A.* **1982**, *79*, 4510.
(8) Ronca, G.; Yoon, D. Y. *J. Chem. Phys.* **1982**, *76*, 3295.
(9) Flory, P. J. *Pure Appl. Chem., Macromol. Chem.* **1972**, *8*, 1. *Faraday Discuss. Chem. Soc.* **1979**, *No. 68*, 14.
(10) See, for example: Cotton, J. P., et al. *Macromolecules* **1974**, *7*, 863. Kirste, R. G.; Kruse, W. A.; Ibel, K. *Polymer* **1975**, *16*, 120. Wignall, G. D.; Ballard, D. G. H.; Schelten, J. *Eur. Polym. J.* **1974**, *10*, 861. Fischer, E. W.; Lieser, G.; Ibel, K. *J. Polym. Sci. Polym. Lett. Ed.* **1975**, *13*, 39.
(11) Flory, P. J. *J. Chem. Phys.* **1949**, *17*, 303.
(12) Flory, P. J. *Proc. R. Soc. London, Ser. A* **1956**, *234*, 73.
(13) Nagle, J. F. *Proc. R. Soc. London, Ser. A* **1974**, *337*, 569.
(14) Gibbs, J. H. *J. Chem. Phys.* **1956**, *25*, 185. DiMarzio, E. A.; Gibbs, J. H. *Ibid.* **1958**, *28*, 807.
(15) Yoon, D. Y.; Baumgartner, A., in preparation.
(16) Gasparoux, H.; Regaya, B.; Priest, J. *C. R. Hebd. Seances Acad. Sci., Ser. B* **1971**, *272*, 1168.
(17) Wissbrun, K. F.; Griffin, A. C. *J. Polym. Sci., Polym. Phys. Ed.* **1982**, *20*, 1835.
(18) Hassner, A.; Alexanian, V. *Tetrahedron Lett.* **1978**, *4475*.
(19) van Meter, J. P.; Klanderman, B, H. *Mol. Cryst. Liq. Cryst.* **1973**, *22*, 271.
(20) Scott, C., private communication.
(21) Flory, P. J. *Ber. Bunsenges. Phys. Chem.* **1977**, *81*, 885.
(22) Mandelkern, L. "Crystallization of Polymers"; McGraw-Hill: New York, 1964.
(23) Flygare, W. H. *Chem. Rev.* **1974**, *74*, 653.
(24) Harkema, S.; Gaymans, R. J.; van Hummel, G. J.; Zylberlicht, D. *Acta Crystallogr., Sect. B* **1979**, *35*, 506.
(25) Hummel, J. P.; Flory, P. J. *Macromolecules* **1980**, *13*, 479.
(26) Goodwin, T. H.; Przybylska, M.; Robertson, J. M. *Acta Crystallogr.* **1950**, *3*, 279. Norment, H. G.; Karle, I. L. *Ibid.* **1962**, *15*, 873.
(27) Jernigan, R. L.; Flory, P. J. *J. Chem. Phys.* **1967**, *47*, 1999.
(28) Flory, P. J. "Statistical Mechanics of Chain Molecules"; Interscience: New York, 1969.
(29) Flory, P. J. *Macromolecules* **1974**, *7*, 381.
(30) This is valid only for polymer. For example, $\chi_{10} = 3\chi_{C-H}$ for the monomer. This difference, however, is very small and hence is neglected here.
(31) Abe, A.; Jernigan, R. L.; Flory, P. J. *J. Am. Chem. Soc.* **1966**, *88*, 631.
(32) Pines, A.; Chang, J. J. *J. Am. Chem. Soc.* **1974**, *96*, 5590.
(33) Volino, F.; Martins, A. F.; Dianoux, A. J. *Mol. Cryst. Liq. Cryst.* **1981**, *66*, 37.
(34) Maier, W.; Saupe, A. *Z. Naturforsch. A* **1959**, *14A*, 882; **1960**, *15A*, 287.